 CMES, vol.101, no.6, pp.421-440, 2014

A Projection Method for the Monolithic Interaction System of an Incompressible Fluid and a Structure using a New Algebraic Splitting

D. Ishihara[1] **and T. Horie**[1]

Abstract: In this study, a projection method for the monolithic interaction system of an incompressible fluid and a structure using a new algebraic splitting is proposed. The proposed method splits the monolithic equation system into the equilibrium equations and the pressure Poisson equation (PPE) algebraically using the intermediate velocity in the nonlinear iterations. Since the proposed equilibrium equation satisfies the interface condition, the proposed method is strongly coupled. Moreover, the proposed PPE enforces the incompressibility constraint. Different from previous studies, the proposed algebraic splitting never generates any Schur complement. The proposed method is applied to a channel with a flexible flap, which is one of typical test problems, where its superior computational efficiencies are demonstrated.

Keywords: Fluid-structure interaction, incompressible fluid, projection method, splitting, monolithic method, strongly coupled.

1 Introduction

Theoretical and experimental difficulties, such as a strong nonlinearity and problems arising during dynamically scaled modeling [Ishihara et al. (2009b)], often appear in the case of fluid-structure interaction (FSI). Therefore, computational mechanics are considered an effective tool for investigating FSI [Taylor and Humphrey (2009); Ishihara et al. (2009a); Takizawa and Tezduyar (2012); Nakata and Liu (2012)]. There are essentially two computational methods for FSI, i.e., the monolithic (simultaneous, direct, or fully coupled) and partitioned methods [Rugonyi and Bathe (2001)].

In the monolithic method, the fluid and structural equations and the interface conditions (comprising geometrical compatibility and equilibrium conditions on the fluid-structure interface) are discretized and solved simultaneously [Zhang and Hisada

[1] Kyushu Institute of Technology, Iizuka, Fukuoka, Japan.

(2001); Hubner et al. (2004)]. Since this formulation enforces the interface conditions, the method is strongly coupled [Fernandez et al. (2007)]. The major drawbacks of the monolithic method are that the formulation can lead to an ill-conditioned equation system [Rugonyi and Bathe (2001); Hubner et al. (2004); Ishihara and Yoshimura (2005); Ishihara et al. (2008)] and that ad hoc code development is required. The straightforward approach addressing the first drawback is preconditioning for the monolithic equation system based on incomplete LU decomposition [Hubner et al. (2004); Washio et al. (2005); Badia et al. (2008b); Badia et al. (2008c)].

In the partitioned method, the fluid and structure are solved separately, and they are coupled via the transmission of their solutions on the interface. The transmission algorithm is usually the Dirichlet–Neumann algorithm, which imposes the Dirichlet and Neumann boundary conditions on the interface for the fluid and the structure, respectively, but other algorithms [Deparis et al. (2008); Badia et al. (2008a)] are also effective. When the interface conditions are not exactly satisfied, the partitioned method is said to be weakly coupled and spurious numerical power on the interface yields numerical instability [Fernandez et al. (2007)]. Therefore, coupled iterations are required for the partitioned method to enforce the interface conditions. Relaxed fixed point iterations are widely used since they allow reuse of existing fluid and structural codes due to the modularity. Nevertheless, relaxed fixed point iterations suffer numerical difficulties [Causin et al. (2005); Forster et al. (2007)], typically including the so-called added mass effect [Le Tallec and Mouro (2001)], such that the convergence of the coupled iterations is too slow or even fails. This type of the numerical difficulty occurs in the cases that the mass density ratio of the fluid and the structure exceeds a certain threshold [Causin et al. (2005)], the domains are considerably constrained [Idelsohn et al. (2009)], and the structure undergoes a large deformation [Dettmer and Peric (2006); Kuttler and Wall (2008)]. These cases are typically seen in light or thin structures in water and in biomechanics applications, such as blood flow in arteries. In these cases, applying dynamic relaxation to fixed point iterations using the line-search technique [Kuttler and Wall (2008); Yamada and Yoshimura (2008)] can lead to some improvement of the convergence speed of the coupled iterations while maintaining the modularity.

As an alternative to fixed point iterations, Newton-type methods have been used to further accelerate the convergence of coupled iterations [Gerbeau and Vidrascu (2003); Matthies and Steindorf (2003); Heil (2004); Fernandez (2005); Dettmer and Peric (2006); Matthies et al. (2006)]. These methods are based on the monolithic equation system [Matthies and Steindorf (2003); Heil (2004); Dettmer and Peric (2006); Matthies et al. (2006)] or the nonlinear fixed point problem [Gerbeau

and Vidrascu (2003); Fernandez (2005)]. In both of these two approaches, linearization and decomposition [Fellipa et al., (2001)] of spatially discretized equations inevitably drive up the cost of the computations. Therefore, the Klyrov method with a preconditioner based on the block-triangular approximation of the Jacobian matrix in Heil (2004) and the Jacobian-free Newton–Klyrov method [Knoll and Keyes (2004)] in Gerbeau and Vidrascu (2003), Matthies and Steindorf (2003), and Matthies et al. (2006) have been successfully used for the approximation of these computations. Nevertheless, a loss of robustness can occur, depending on the degree of the approximation [Heil (2004); Zhang and Hisada (2004); Fernandez (2005); Minami and Yoshimura (2010)]. Loss of robustness is also an important issue for projection methods applied to the FSI described below, since these methods usually use splitting of spatially discretized equations or algebraic splitting.

That the added mass effect seems to arise from the fluid incompressibility constraint is important in the design of the stable and efficient computational methods for the FSI [Causin et al. (2005)]. Fernandez at al. (2007) is one of the studies that explicitly take this into account, where the splitting of the equation system is performed at the continuous problem level (continuous splitting) using a projection method in the fluid [Chorin (1968)]. The projection method has been successfully used for an incompressible fluid, due to the method's computational efficiency [Codina (2001)], where the equation system is split into the equilibrium equations and the pressure Poisson equation (PPE), which enforces the incompressibility constraint. Therefore, it is expected that this type of method is also effective for the FSI including fluid incompressibility. There exist other projection methods applied to the FSI that use algebraic splitting based on block-LU factorization [Badia et al. (2008b); Badia et al. (2008c)] or substructuring [Ishihara and Yoshimura (2005); Ishihara et al. (2008); Idelsohn et al. (2009)]. Nevertheless, their algebraic splitting produces the Schur complement inevitably. Therefore, its approximation is necessary required for computational efficiency [Badia et al. (2008b); Badia et al. (2008c); Idelsohn et al. (2009)].

In this study, a projection method for the monolithic interaction system of an incompressible fluid and a structure using a new algebraic splitting is proposed. In the nonlinear iterations, the monolithic equation system is split into the equilibrium equations and the PPE algebraically using the intermediate state variables. Since the proposed equilibrium equations satisfy the interface condition, the proposed method is strongly coupled. Moreover, the PPE enforces the incompressibility constraint. Different from the previous studies, the proposed algebraic splitting never produces any Schur complement. The proposed method is applied for a channel with a flexible flap [Mok and Wall (2001); Neumann et al. (2006)], which is one of typical test problems, in order to demonstrate its computational efficiencies.

2 Monolithic interaction system of an incompressible fluid and a flexible structure

2.1 Governing equations

Ω_t^{f} and Ω_t^{s} denote the spatial domains of the fluid and the elastic structure at time t, respectively, and Γ_t^{fs} denotes the fluid–structure interface at time t. The superscripts f, s, and fs indicate quantities corresponding to the fluid, structure, and fluid–structure interface, respectively. The arbitrary Lagrangian–Eulerian (ALE) method [Hughes et al. (1981)] is used to describe the fluid motion in the deformable domain. The ALE form of the incompressible Navier–Stokes equations can be expressed as

$$\rho^{\mathrm{f}}\frac{\partial v_i^{\mathrm{f}}}{\partial t}+\rho^{\mathrm{f}}(v_j^{\mathrm{f}}-v_j^{\mathrm{m}})\frac{\partial v_i^{\mathrm{f}}}{\partial x_j}=\frac{\partial \sigma_{ji}^{\mathrm{f}}}{\partial x_j}+\rho^{\mathrm{f}}g_i^{\mathrm{f}}, \tag{1a}$$

and

$$\frac{\partial v_i^{\mathrm{f}}}{\partial x_i}=0, \tag{1b}$$

in Ω_t^{f}, where ρ^{f} is the mass density of the fluid, v_i^{f} is the ith component of the fluid velocity vector, v_i^{m} is the ith component of the velocity vector of the ALE coordinate, σ_{ij}^{f} is the ijth component of the Cauchy stress tensor of the fluid, and g_i^{f} is the ith component of the body force vector acting on the fluid. The fluid is assumed to be Newtonian.

The equilibrium equation of the elastic structure is expressed as

$$\rho^{\mathrm{s}}\frac{\mathrm{d}^2u_i^{\mathrm{s}}}{dt^2}=\frac{\partial \sigma_{ji}^{\mathrm{s}}}{\partial x_j}+\rho^{\mathrm{s}}g_i^{\mathrm{s}}, \tag{2}$$

in Ω_t^{s}, where ρ^{s} is the mass density of the structure, u_i^{s} is the ith component of the structural displacement vector, σ_{ij}^{s} is the ijth component of the Cauchy stress tensor of the structure, and g_i^{s} is the ith component of the body force vector acting on the structure. The strains remain small, although the structure undergoes finite deformations. Therefore, a linear elastic material is assumed.

The following geometrical compatibility and equilibrium conditions (the interface conditions) are imposed on the fluid–structure interface:

The geometrical compatibility condition as

$$v_i^{\mathrm{f}}=v_i^{\mathrm{s}}, \tag{3a}$$

and the equilibrium condition as

$$\sigma_{ij}^{\mathrm{f}} n_j^{\mathrm{f}} + \sigma_{ij}^{\mathrm{s}} n_j^{\mathrm{s}} = 0, \tag{3b}$$

on Γ_t^{fs}, where v_i^{s} is the ith component of the structural velocity vector, and n_i^{f} and n_i^{s} are the ith components of the outward unit normal vectors corresponding to the fluid and the structure, respectively.

2.2 Space discretization

The space discretizations are performed in advance to avoid pressure boundary condition problems associated with the splitting of the continuous problem [Perot (1993)]. Applying finite element discretization to the equations (1a) and (1b), the following nonlinear equation system can be obtained in matrix form:

The equilibrium equation as

$$\mathbf{Q}^{\mathrm{f}} \equiv {}_{\mathrm{L}}\mathbf{M}^{\mathrm{f}}\mathbf{a}^{\mathrm{f}} + \mathbf{C}^{\mathrm{f}}\mathbf{v}^{\mathrm{f}} + \mathbf{N}^{\mathrm{f}} - \mathbf{G}^{\mathrm{f}}\mathbf{p}^{\mathrm{f}} = \mathbf{g}^{\mathrm{f}}, \tag{4a}$$

and the incompressibility constraint as

$$_{\tau}\mathbf{G}^{\mathrm{f}}\mathbf{v}^{\mathrm{f}} = \mathbf{0}, \tag{4b}$$

where $\mathbf{M}^{\mathrm{f}}$ is the mass matrix of the fluid, $\mathbf{C}^{\mathrm{f}}$ is the diffusive matrix of the fluid, $\mathbf{N}^{\mathrm{f}}$ is the convective term vector of the fluid, $\mathbf{G}^{\mathrm{f}}$ is the divergence operator matrix of the fluid, $\mathbf{g}^{\mathrm{f}}$ is the external force vector acting on the fluid, $\mathbf{a}^{\mathrm{f}}$ is the acceleration vector of the fluid, $\mathbf{v}^{\mathrm{f}}$ is the velocity vector of the fluid, $\mathbf{p}^{\mathrm{f}}$ is the pressure vector of the fluid, $\mathbf{Q}^{\mathrm{f}}$ is the internal force vector including all effects of the fluid, the subscript L indicates the lumping of the matrix, and the subscript τ indicates the transpose of the matrix.

Applying finite element discretization to the total Lagrangian formulation of the equation (2), the following nonlinear equation system can be obtained in matrix form:

The equilibrium equation as

$$\mathbf{Q}^{\mathrm{s}} \equiv {}_{\mathrm{L}}\mathbf{M}^{\mathrm{s}}\mathbf{a}^{\mathrm{s}} + \mathbf{q}^{\mathrm{s}}(\mathbf{u}^{\mathrm{s}}) = \mathbf{g}^{\mathrm{s}}, \tag{5}$$

where $\mathbf{M}^{\mathrm{s}}$ is the mass matrix of the structure, $\mathbf{q}^{\mathrm{s}}$ is the elastic internal force vector of the structure, $\mathbf{g}^{\mathrm{s}}$ is the external force vector acting on the structure, $\mathbf{a}^{\mathrm{s}}$ is the acceleration vector of the structure, $\mathbf{u}^{\mathrm{s}}$ is the displacement vector of the structure, and $\mathbf{Q}^{\mathrm{s}}$ is the internal force vector including all effects of the structure. The finite deformation is taken into account using the total Lagrangian formulation, where

the Hooke's law is used for the relation between the second Piola-Kirchhoff stress and the Green-Lagrange strain under the assumption of small strain.

The interface conditions (3a) and (3b) can be rewritten in vector form as, respectively,

$$\mathbf{v}_c^{\mathrm{fs}} \equiv \mathbf{v}_c^{\mathrm{f}} = \mathbf{v}_c^{\mathrm{s}}, \tag{6a}$$

and

$$\mathbf{Q}_c^{\mathrm{f}} + \mathbf{Q}_c^{\mathrm{s}} = \mathbf{g}_c^{\mathrm{fs}}, \tag{6b}$$

where the subscript c indicates the coupled degrees of freedoms (DOFs).

The spatially discretized governing equations (4), (5), and (6) can be rewritten as the following monolithic equation system:

The equilibrium equation as

$$\mathbf{Q} \equiv {}_{\mathrm{L}}\mathbf{M}\mathbf{a} + \mathbf{C}\mathbf{v} + \mathbf{N} + \mathbf{q}(\mathbf{u}) - \mathbf{G}\mathbf{p} = \mathbf{g}, \tag{7a}$$

and the incompressibility constraint as

$$\tau\mathbf{G}\mathbf{v} = \mathbf{0}, \tag{7b}$$

where the matrices and the vectors appearing in these equations are defined as

$${}_{\mathrm{L}}\mathbf{M} \equiv \begin{bmatrix} {}_{\mathrm{L}}\mathbf{M}_{ii}^{\mathrm{f}} & \mathbf{0} & \mathbf{0} \\ \mathbf{0} & {}_{\mathrm{L}}\mathbf{M}_{cc}^{\mathrm{fs}} & \mathbf{0} \\ \mathbf{0} & \mathbf{0} & {}_{\mathrm{L}}\mathbf{M}_{ii}^{\mathrm{s}} \end{bmatrix}, \quad \mathbf{C} \equiv \begin{bmatrix} \mathbf{C}_{ii}^{\mathrm{f}} & \mathbf{C}_{ic}^{\mathrm{f}} & \mathbf{0} \\ \mathbf{C}_{ci}^{\mathrm{f}} & \mathbf{C}_{cc}^{\mathrm{f}} & \mathbf{0} \\ \mathbf{0} & \mathbf{0} & \mathbf{0} \end{bmatrix}, \quad \mathbf{G} \equiv \begin{bmatrix} \mathbf{G}_i^{\mathrm{f}} \\ \mathbf{G}_c^{\mathrm{f}} \\ \mathbf{0} \end{bmatrix},$$

$$\mathbf{N} \equiv \begin{Bmatrix} \mathbf{N}_i^{\mathrm{f}} \\ \mathbf{N}_c^{\mathrm{f}} \\ \mathbf{0} \end{Bmatrix}, \quad \mathbf{q}(\mathbf{u}) \equiv \begin{Bmatrix} \mathbf{0} \\ \mathbf{q}_c^{\mathrm{s}}(\mathbf{u}^{\mathrm{s}}) \\ \mathbf{q}_i^{\mathrm{s}}(\mathbf{u}^{\mathrm{s}}) \end{Bmatrix}, \quad \mathbf{g} \equiv \begin{Bmatrix} \mathbf{g}_i^{\mathrm{f}} \\ \mathbf{g}_c^{\mathrm{fs}} \\ \mathbf{g}_i^{\mathrm{s}} \end{Bmatrix},$$

$$\mathbf{a} \equiv \begin{Bmatrix} \mathbf{a}_i^{\mathrm{f}} \\ \mathbf{a}_c^{\mathrm{fs}} \\ \mathbf{a}_i^{\mathrm{s}} \end{Bmatrix}, \quad \mathbf{v} \equiv \begin{Bmatrix} \mathbf{v}_i^{\mathrm{f}} \\ \mathbf{v}_c^{\mathrm{fs}} \\ \mathbf{v}_i^{\mathrm{s}} \end{Bmatrix}, \quad \mathbf{u} \equiv \begin{Bmatrix} * \\ \mathbf{u}_c^{\mathrm{fs}} \\ \mathbf{u}_i^{\mathrm{s}} \end{Bmatrix}, \quad \mathbf{p} \equiv \mathbf{p}^{\mathrm{f}},$$

$${}_{\mathrm{L}}\mathbf{M}_{cc}^{\mathrm{fs}} \equiv {}_{\mathrm{L}}\mathbf{M}_{cc}^{\mathrm{f}} + {}_{\mathrm{L}}\mathbf{M}_{cc}^{\mathrm{s}}, \tag{8a-k}$$

in which the the subscript i indicates uncoupled DOFs.

3 Formulation of the proposed projection method

3.1 Monolithic method

The projection method using the algebraic splitting in this study as well as those in prior studies [Ishihara and Yoshimura (2005); Ishihara et al. (2008); Badia et al. (2008b); Badia et al. (2008c); Idelsohn et al. (2009)] is based on the monolithic method that solves the equilibrium equation (7a) and the incompressibility constraint (7b) simultaneously, the details of which are described as follows:

In order to linearize and solve the nonlinear equation system (7) iteratively (the nonlinear iterations), let us use the following increments of the state variables from the previous iteration $k-1$ to the current iteration k:

$$^{t+\Delta t}\mathbf{a}^{(k)} = ^{t+\Delta t}\mathbf{a}^{(k-1)} + \Delta\mathbf{a}, \tag{9a}$$

$$^{t+\Delta t}\mathbf{v}^{(k)} = ^{t+\Delta t}\mathbf{v}^{(k-1)} + \Delta\mathbf{v} = ^{t+\Delta t}\mathbf{v}^{(k-1)} + \gamma\Delta t\Delta\mathbf{a}, \tag{9b}$$

$$^{t+\Delta t}\mathbf{u}^{(k)} = ^{t+\Delta t}\mathbf{u}^{(k-1)} + \Delta\mathbf{u} = ^{t+\Delta t}\mathbf{u}^{(k-1)} + \beta\Delta t^2\Delta\mathbf{a}, \tag{9c}$$

$$^{t+\Delta t}\mathbf{p}^{(k)} = ^{t+\Delta t}\mathbf{p}^{(k-1)} + \Delta\mathbf{p}, \tag{9d}$$

where $\mathbf{a}$, $\mathbf{v}$, $\mathbf{u}$, and $\mathbf{p}$ denote the acceleration, the velocity, the displacement, and the pressure, respectively, Δ denotes the increment, $t+\Delta t$ denotes the current time, and the relations between these increments are given as $\Delta\mathbf{u} = \beta\Delta t^2\Delta\mathbf{a}$ and $\Delta\mathbf{v} = \gamma\Delta t\Delta\mathbf{a}$ based on Newmark's β method.

The monolithic equation system (7) is linearized using the relations (9a) - (9d) to obtain the following equations:

$$\mathbf{M}^*\Delta\mathbf{a} - \mathbf{G}\Delta\mathbf{p} = \Delta\mathbf{g}, \tag{10a}$$

$$\gamma\Delta t\,_\tau\mathbf{G}\Delta\mathbf{a} + \mathbf{G}_\varepsilon\Delta\mathbf{p} = \Delta\mathbf{h}, \tag{10b}$$

where the pressure term and the elastic interior force term are evaluated implicitly, $\mathbf{M}^*$is the generalized mass matrix, $\Delta\mathbf{g}$ and $\Delta\mathbf{h}$ are the residual vectors of the equilibrium equation (7a) and the incompressibility constraint (7b), respectively, Δt is the time increment, and $\mathbf{G}_\varepsilon$ is come from the pressure stabilization term of the PSPG method [Tedzduyar et al. (1992)]. Note that the definition of $\mathbf{M}^*$ depends on the evaluations of the fluid convection and diffusion terms as follows:

(Definition 1) If the fluid convection and diffusion terms are evaluated implicitly,

$$\mathbf{M}^* \equiv {}_\mathrm{L}\mathbf{M} + \gamma\Delta t(\tilde{\mathbf{N}} + \mathbf{C}) + \beta\Delta t^2\mathbf{K}, \tag{11}$$

where $\tilde{\mathbf{N}}$ is defined as

$$\tilde{\mathbf{N}} = \begin{bmatrix} \tilde{\mathbf{N}}^{\mathrm{f}}_{ii} & \tilde{\mathbf{N}}^{\mathrm{f}}_{ci} & \mathbf{0} \\ \tilde{\mathbf{N}}^{\mathrm{f}}_{ic} & \tilde{\mathbf{N}}^{\mathrm{f}}_{cc} & \mathbf{0} \\ \mathbf{0} & \mathbf{0} & \mathbf{0} \end{bmatrix}, \tag{12}$$

where $\tilde{\mathbf{N}}^{\mathrm{f}}$ is the Jacobian of $\mathbf{N}^{\mathrm{f}}$, and $\mathbf{K}$ is defined using the tangential stiffness matrix of the structure $\mathbf{K}^{\mathrm{s}}$, which is the Jacobian of $\mathbf{q}^{\mathrm{s}}$, as

$$\mathbf{K} = \begin{bmatrix} \mathbf{0} & \mathbf{0} & \mathbf{0} \\ \mathbf{0} & \mathbf{K}^{\mathrm{s}}_{cc} & \mathbf{K}^{\mathrm{s}}_{ci} \\ \mathbf{0} & \mathbf{K}^{\mathrm{s}}_{ic} & \mathbf{K}^{\mathrm{s}}_{ii} \end{bmatrix}. \tag{13}$$

(Definition 2) If the fluid convection term is evaluated explicitly, while the fluid diffusive term is evaluated implicitly,

$$\mathbf{M}^{*} \equiv {}_{\mathrm{L}}\mathbf{M} + \gamma\Delta t\mathbf{C} + \beta\Delta t^{2}\mathbf{K}. \tag{14}$$

(Definition 3) If the fluid convection and diffusion terms are evaluated explicitly,

$$\mathbf{M}^{*} \equiv {}_{\mathrm{L}}\mathbf{M} + \beta\Delta t^{2}\mathbf{K}. \tag{15}$$

In the definition 2, the following necessary condition is imposed on the time increment Δt for the stability of the time integration:

Courant's number condition as

$$V^{\mathrm{f}}\Delta t/\Delta h^{\mathrm{f}} < 1, \tag{16}$$

where V^{f} is the characteristic fluid velocity, Δh^{f} is the minimum size of fluid elements.

In the definition 3, both of the necessary condition (16) and the following necessary condition are imposed on the time increment Δt for the stability of the time integration:

Diffusion number condition as

$$(\mu^{\mathrm{f}}/\rho^{\mathrm{f}})\Delta t/\Delta h^{\mathrm{f}2} < 1/2, \tag{17}$$

where μ^{f} is the fluid viscosity.

In the standard monolithic method, the following simultaneous equation system that consists of equations (10a) and (10b) is solved:

$$\begin{bmatrix} \mathbf{M}^{*} & -\mathbf{G} \\ \gamma\Delta t_{\tau}\mathbf{G} & \mathbf{G}_{\varepsilon} \end{bmatrix} \begin{Bmatrix} \Delta\mathbf{a} \\ \Delta\mathbf{p} \end{Bmatrix} = \begin{Bmatrix} \Delta\mathbf{g} \\ \Delta\mathbf{h} \end{Bmatrix}. \tag{18}$$

The example of the coefficient matrix (18) can be written as follows:

$$\begin{bmatrix} {}_{\mathrm{L}}\mathbf{M}^{\mathrm{f}}_{ii} & \mathbf{0} & \mathbf{0} & -\mathbf{G}^{\mathrm{f}}_{i} \\ \mathbf{0} & {}_{\mathrm{L}}\mathbf{M}^{\mathrm{fs}}_{cc}+\beta\Delta t^2\mathbf{K}^{\mathrm{s}}_{cc} & \beta\Delta t^2\mathbf{K}^{\mathrm{s}}_{ci} & -\mathbf{G}^{\mathrm{f}}_{c} \\ \mathbf{0} & \beta\Delta t^2\mathbf{K}^{\mathrm{s}}_{ic} & {}_{\mathrm{L}}\mathbf{M}^{\mathrm{s}}_{ii}+\beta\Delta t^2\mathbf{K}^{\mathrm{s}}_{ii} & \mathbf{0} \\ \gamma\Delta t_\tau\mathbf{G}^{\mathrm{f}}_{i} & \gamma\Delta t_\tau\mathbf{G}^{\mathrm{f}}_{c} & \mathbf{0} & \mathbf{G}_{\varepsilon} \end{bmatrix}, \tag{19}$$

where the definition 3 of $\mathbf{M}^*$ is used.

The predictor-multicorrector algorithm (PMA) for the FSI [Zhang and Hisada (2001)] is used for the time integration. The loop of the iterative procedure corresponds to the multicorrection loop of PMA and the relation (9) corresponds to the corrector of the PMA. The predictor of the PMA is provided using Newmark's β method as

$${}^{t+\Delta t}\mathbf{a}^{(0)} = \mathbf{0}, \tag{20a}$$

$${}^{t+\Delta t}\mathbf{v}^{(0)} = {}^{t}\mathbf{v} + \Delta t(1-\gamma){}^{t}\mathbf{a}, \tag{20b}$$

$${}^{t+\Delta t}\mathbf{u}^{(0)} = {}^{t}\mathbf{u} + \Delta t\,{}^{t}\mathbf{v} + \Delta t^2(1/2-\beta){}^{t}\mathbf{a}, \tag{20c}$$

$${}^{t+\Delta t}\mathbf{p}^{(0)} = {}^{t}\mathbf{p}, \tag{20d}$$

where ${}^{t}\mathbf{a}$, ${}^{t}\mathbf{v}$, ${}^{t}\mathbf{u}$, and ${}^{t}\mathbf{p}$ are the known acceleration, velocity, displacement, and pressure that are obtained in the previous time step t.

3.2 Projection method

When the interface conditions are not exactly satisfied, spurious numerical power on the interface yields numerical instability [Fernandez et al. (2007)]. The monolithic method satisfies the interface conditions and is strongly coupled. However, the formulation leads to an ill-conditioned monolithic equation system [Rugonyi and Bathe (2001); Hubner et al. (2004); Ishihara and Yoshimura (2005); Ishihara et al. (2008)]. In the projection methods [Badia et al. (2008b); Badia et al. (2008c); Ishihara and Yoshimura (2005); Ishihara et al. (2008); Idelsohn et al. (2009)], the monolithic equation system is split into its subsystems algebraically. Therefore, the ill-condition of the monolithic equation system will be reduced. Their algebraic splitting is based on block-LU factorization [Badia et al. (2008b); Badia et al. (2008c)] or substructuring [Ishihara and Yoshimura (2005); Ishihara et al. (2008); Idelsohn et al. (2009)] that produces the Schur complement inevitably. Therefore, a major concern in these studies is how to approximate the Schur complement without loss of robustness [Heil (2004); Zhang and Hisada (2004); Fernandez (2005); Idelsohn et al. (2009); Minami and Yoshimura (2010)]. The proposed method differs from those in these prior studies, the details of which are described as follows:

The state variables is predicted as the intermediate state variables from the equilibrium equation (7a) for the known pressure ${}^{t+\Delta t}\mathbf{p}^{(k-1)}$, which is linearized as

$$\mathbf{M}^*\Delta\hat{\mathbf{a}} = \Delta\mathbf{g}, \tag{21}$$

where the intermediate state variables and their increments are defined as

$${}^{t+\Delta t}\hat{\mathbf{a}}^{(k)} = {}^{t+\Delta t}\mathbf{a}^{(k-1)} + \Delta\hat{\mathbf{a}}, \tag{22a}$$

$${}^{t+\Delta t}\hat{\mathbf{v}}^{(k)} = {}^{t+\Delta t}\mathbf{v}^{(k-1)} + \Delta\hat{\mathbf{v}} = {}^{t+\Delta t}\mathbf{v}^{(k-1)} + \gamma\Delta t\Delta\hat{\mathbf{a}}, \tag{22b}$$

$${}^{t+\Delta t}\hat{\mathbf{u}}^{(k)} = {}^{t+\Delta t}\mathbf{u}^{(k-1)} + \Delta\hat{\mathbf{u}} = {}^{t+\Delta t}\mathbf{u}^{(k-1)} + \beta\Delta t^2\Delta\hat{\mathbf{a}}, \tag{22c}$$

where $\hat{\mathbf{a}}$, $\hat{\mathbf{v}}$ and $\hat{\mathbf{u}}$ are the intermediate acceleration, velocity and displacement, respectively, and they are the predictions of the acceleration, velocity and displacement, respectively.

Subtracting both sides of equation (21) from those of equation (10a) and similarly subtracting equation (22b) from equation (9b) and substituting the result into the first difference gives, after suitable rearrangement,

$$\gamma\Delta t\mathbf{G}\Delta\mathbf{p} = \mathbf{M}^*\left({}^{t+\Delta t}\mathbf{v}^{(k)} - {}^{t+\Delta t}\hat{\mathbf{v}}^{(k)}\right). \tag{23}$$

Left multiplying both sides of equation (23) by ${}_\tau\mathbf{G}_\mathrm{L}\mathbf{M}^{-1}$, the following equation is obtained:

$$\begin{aligned}\gamma\Delta t\,{}_\tau\mathbf{G}_\mathrm{L}\mathbf{M}^{-1}\mathbf{G}\Delta\mathbf{p} &= {}_\tau\mathbf{G}^{t+\Delta t}\mathbf{v}^{(k)} - {}_\tau\mathbf{G}^{t+\Delta t}\hat{\mathbf{v}}^{(k)} \\ &+ {}_\tau\mathbf{G}_\mathrm{L}\mathbf{M}^{-1}\bar{\mathbf{M}}^*\left({}^{t+\Delta t}\mathbf{v}^{(k)} - {}^{t+\Delta t}\hat{\mathbf{v}}^{(k)}\right)\end{aligned}, \tag{24}$$

where the matrix $\bar{\mathbf{M}}^*$ equals $\mathbf{M}^* - {}_\mathrm{L}\mathbf{M}$.

It is shown from equation (24) that the incompressibility constraint (7b) for the unknown fluid velocity ${}^{t+\Delta t}\mathbf{v}^{(k)}$ is satisfied solving the following PPE:

$$\gamma\Delta t\,{}_\tau\mathbf{G}_\mathrm{L}\mathbf{M}^{-1}\mathbf{G}\Delta\mathbf{p} = -{}_\tau\mathbf{G}^{t+\Delta t}\hat{\mathbf{v}}^{(k)}. \tag{25}$$

If the PPE (25) is solved, then equation (24) is reduced as

$${}_\tau\mathbf{G}^{t+\Delta t}\mathbf{v}^{(k)} + {}_\tau\mathbf{G}_\mathrm{L}\mathbf{M}^{-1}\bar{\mathbf{M}}^*\left({}^{t+\Delta t}\mathbf{v}^{(k)} - {}^{t+\Delta t}\hat{\mathbf{v}}^{(k)}\right) = \mathbf{0}. \tag{26}$$

The intermediate or predicted velocity ${}^{t+\Delta t}\hat{\mathbf{v}}^{(k)}$ satisfies the equilibrium equation (7a) for the previous pressure ${}^{t+\Delta t}\mathbf{p}^{(k-1)}$, while the velocity ${}^{t+\Delta t}\mathbf{v}^{(k)}$ satisfies that for the current pressure ${}^{t+\Delta t}\mathbf{p}^{(k)}$. Therefore, when the present nonlinear iterations are convergent, ${}^{t+\Delta t}\hat{\mathbf{v}}^{(k)}$ agrees with ${}^{t+\Delta t}\mathbf{v}^{(k)}$ asymptotically as

$$\left|{}^{t+\Delta t}\mathbf{v}^{(k)} - {}^{t+\Delta t}\hat{\mathbf{v}}^{(k)}\right| \to 0 \quad \text{as} \quad k \to \infty. \tag{27}$$

Since the nonlinear iterations using the definition (11) are the Newton type iteration, it is convergent in a quadratic way, while the linear convergence is expected for the definition (14) or the definition (15). Therefore, the second term of equation (26) will vanish asymptotically, and the incompressibility constraint for the current fluid velocity is satisfied as follows:

$$\tau \mathbf{G}^{t+\Delta t}\mathbf{v}^{(k)} = \mathbf{0}. \tag{28}$$

It follows from the above formulation that the monolithic equation system is split into the equilibrium equations (21) and (10a) and the PPE (25) using the proposed algebraic splitting, where the intermediate velocity is used and, different from the previous studies using block-LU factorization or substructuring, the Schur complement matrix is never produced.

The proposed method is summarized as follows:

Step 1: The increment of the intermediate acceleration $\Delta\hat{\mathbf{a}}$ is derived from the linearized equilibrium equation for the previous pressure ${}^{t+\Delta t}\mathbf{p}^{(k-1)}$ (21) and then the intermediate velocity ${}^{t+\Delta t}\hat{\mathbf{v}}^{(k)}$ is obtained from equation (22b).

Step 2: The pressure increment $\Delta\mathbf{p}$ is derived from equation (25).

Step 3: The acceleration increment $\Delta\mathbf{a}$ is derived from the linearized equilibrium equation for the current pressure ${}^{t+\Delta t}\mathbf{p}^{(k)}$ (10a) and then the acceleration ${}^{t+\Delta t}\mathbf{a}^{(k)}$, the velocity ${}^{t+\Delta t}\mathbf{v}^{(k)}$, and the displacement ${}^{t+\Delta t}\mathbf{u}^{(k)}$ are obtained from equation (9).

3.3 Partitioning of equilibrium equations using explicit evaluation

For further computational efficiency, we partitioned the equilibrium equation into the fluid interior part and the structural part using the explicit evaluation of the fluid convective and diffusive terms. Note that the structural part includes the fluid-structure interface to satisfy the interface conditions. Let us use the definition (15); then, the fluid interior DOFs of $\mathbf{M}^*$ is reduced to the diagonal matrix. Therefore, the equilibrium equations (10a) and (21) can be partitioned into its fluid interior part and the structural part without any algebraic operation. For example, the equilibrium equation (21) can be partitioned into

$${}_{\mathrm{L}}\mathbf{M}^{\mathrm{f}}_{ii}\Delta\hat{\mathbf{a}}^{\mathrm{f}}_{i} = \Delta\mathbf{g}^{\mathrm{f}}_{i} \tag{29a}$$

and

$$\begin{bmatrix} {}_{\mathrm{L}}\mathbf{M}^{\mathrm{fs}}_{cc} + \beta\Delta t^2\mathbf{K}^{\mathrm{s}}_{cc} & \beta\Delta t^2\mathbf{K}^{\mathrm{s}}_{ci} \\ \beta\Delta t^2\mathbf{K}^{\mathrm{s}}_{ic} & {}_{\mathrm{L}}\mathbf{M}^{\mathrm{s}}_{ii} + \beta\Delta t^2\mathbf{K}^{\mathrm{s}}_{ii} \end{bmatrix} \begin{Bmatrix} \Delta\hat{\mathbf{a}}^{\mathrm{fs}}_{c} \\ \Delta\hat{\mathbf{a}}^{\mathrm{s}}_{i} \end{Bmatrix} = \begin{Bmatrix} \Delta\mathbf{g}^{\mathrm{fs}}_{c} \\ \Delta\mathbf{g}^{\mathrm{s}}_{i} \end{Bmatrix}. \tag{29b}$$

Since the coefficient matrix (29a) is diagonal, the solution can be easily obtained. The present partitioning reduces the computational cost dramatically when the fluid's number of DOFs becomes large.

3.4 Algebraic characteristics of equations

Since the mass density of the fluid is mostly smaller than or comparable to that of the structure, the algebraic characteristic of the coefficient matrix (29b) is similar to the structural generalized mass matrix. The coefficient matrix of the PPE (25) can be rewritten as

$$\gamma\Delta t[\tau\mathbf{G}^{\mathrm{f}}{}_{i\mathrm{L}}\mathbf{M}^{\mathrm{f}-1}_{ii}\mathbf{G}^{\mathrm{f}}{}_{i}+\tau\mathbf{G}^{\mathrm{f}}{}_{c}({}_{\mathrm{L}}\mathbf{M}^{\mathrm{f}}{}_{cc}+{}_{\mathrm{L}}\mathbf{M}^{\mathrm{s}}{}_{cc})^{-1}\mathbf{G}^{\mathrm{f}}{}_{c}]. \tag{30}$$

Let us assume a uniform mesh division, then, the components of the matrix (30) are proportional to $1/\rho^{\mathrm{f}}$ or $1/\rho^{\mathrm{f}}+1/(\rho^{\mathrm{f}}+\rho^{\mathrm{s}})$. These terms have a relationship of $1/\rho^{\mathrm{f}} < 1/\rho^{\mathrm{f}}+1/(\rho^{\mathrm{f}}+\rho^{\mathrm{s}}) < 2/\rho^{\mathrm{f}}$. Therefore, the components of the matrix (30) are almost homogeneous irrespective of the material properties and the time increment. On the other hand, the ill-conditioned coefficient matrix for the monolithic equation system (19) can result since the differences among the coefficient matrix components are quite sensitive to the material properties and the time increment [Rugonyi and Bathe (2001); Hubner, Walhorn and Dinkler (2004); Ishihara and Yoshimura (2005); Washio et al. (2005); Ishihara et al. (2008)].

4 Numerical example

4.1 Problem setup

The proposed method is applied for the channel with a flexible flap shown in Fig. 1 [Mok and Wall (2001)] in order to discuss its convergence properties and computational efficiencies. This problem is known as one of typical problems in order to test the convergence and stability performances of partitioned methods, some of which suffer from the numerical troubles of non-convergent coupled iterations and even instability [Mok and Wall (2001); Neumann et al. (2006); Minami and Yoshimura (2010)]. The flexible flap is fixed in the channel with a slope, as sketched in Fig. 1. The mass density and the Young's modulus of the flap are $\rho^{\mathrm{s}} = 1500$ kg/m^3 and $E^{\mathrm{s}} = 2.3\times10^6$ Pa, respectively. The mass density and the viscosity of the fluid are $\rho^{\mathrm{f}} = 956$ kg/m^3 and $\mu^{\mathrm{f}} = 0.145$ kg/(m·s), respectively. As shown in Fig. 1, the inlet velocity has a parabolic profile and its velocity at the top v_{in} is given as V_{in} (1-cos2πft)/2 ($V_{\mathrm{in}} = 0.06067$ m/sec and $f = 0.05$ Hz) until 10 sec and V_{in} after 10 sec.

The critical time increment Δt_c is given as approximately 0.4 sec from the Courant number condition (16), where the characteristic fluid velocity V^{f} is defined as the maximum inlet velocity V_{in}, and the minimum fluid element size Δh^{f} is 0.025 m. The structural mesh of the flap consists of shell elements using a mixed interpolation of tensorial components (MITC) [Bathe and Dvorkin (1985); Noguchi and

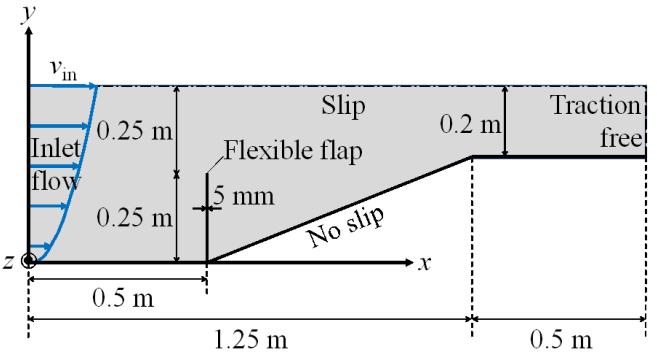

Figure 1: Setup of the flexible flap in the channel with a slope

Hisada (1993)] (22 nodes and 10 elements), while the fluid mesh of the channel consists of P1P1 elements [Tedzduyar et al. (1992)] (2,982 nodes and 8,400 elements). The Streamline-Upwind Petrov-Galerkin (SUPG)/PSPG method [Tedzduyar et al. (1992)] is used for the stability of the fluid analysis. This problem is two-dimensional, as shown in Fig. 1. Therefore, the analysis is restricted within the *xy* plane, i.e., there is a single division of the fluid and structural meshes in the *z* direction, no rotation around the *y* direction and no translation in the z direction of the flap, and no inlet or outlet flow in the z direction.

The coefficient matrices of the equations (10a), (21) and (25) are symmetric and positive definite. Therefore, these equations are solved by the conjugate gradient (CG) method with diagonal scaling, while Eq. (18) is solved by the biconjugate gradient stabilized (BiCGSTAB) method with diagonal scaling. The iterations are repeated until the current residual norm reaches 0.0001 % of the initial residual norm.

4.2 Results and discussion

First, we present the convergence properties of the iterative solvers. Fig. 2 shows the relationship between the time increment Δt and the number of the iterations of the iterative solvers at the first time step. As shown in Fig. 2, the convergence property of the iterative solver in the monolithic method becomes drastically worse as Δtincreases. Moreover, in the case using Δt larger than approximately 0.11sec, the iterations failed to converge. On the other hand, those in the proposed method are stable irrespective of Δt due to the algebraic characteristics discussed in Section 3.4. It follows from this result that the proposed method is computationally efficient.

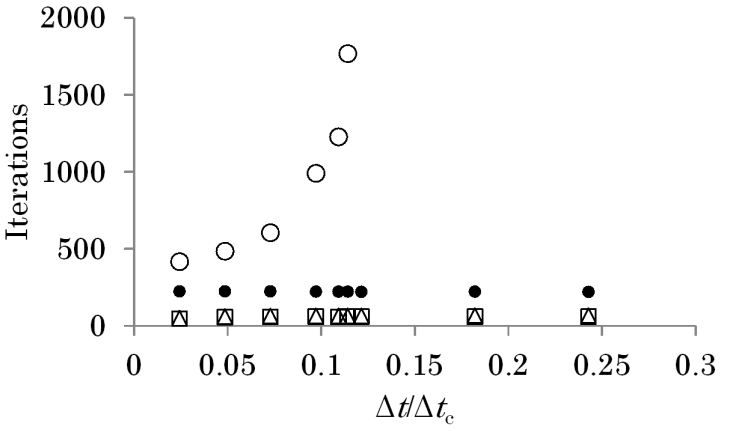

Figure 2: Convergence properties of the iterative solvers. The white circles indicate the result for the monolithic equation system (18), the black circles indicate the result for the pressure Poisson equation (25), the squares indicate the result for the equilibrium equation (21), and the triangles indicate the result for the equilibrium equation (10a).

Next, we present the convergence property of the nonlinear iterations. Here, Δt is fixed at 0.1 sec, which is approximately $\Delta t_c/4$, because it was typically used in the previous studies. Fig. 3 shows the transition of the difference between the intermediate velocity and the velocity in the nonlinear iteration at the first time step, where we defined the difference as

$$\sum_{i=1}^{ndofs} \left| {}^{t+\Delta t}\hat{v}_i^{(k)} - {}^{t+\Delta t}v_i^{(k)} \right| / \sum_{i=1}^{ndofs} \left| {}^{t+\Delta t}v_i^{(k)} \right|. \tag{31}$$

Here, *ndofs* is the total number of DOFs, and *i* indexes the DOF. As shown in Fig. 3, this difference linearly converged, as discussed in Section 3.2. Therefore, the PPE (25) was solved so as to satisfy the incompressibility constraint asymptotically for the current fluid velocity (28), as proven by the relation (26).

Finally, we present the number of the nonlinear iterations in order to obtain the convergent solution. Again, Δt is fixed to 0.1 sec. The computation was executed for the complete analysis period with the number of nonlinear iterations fixed at one, two, or three. Fig. 4 shows time histories for the x displacement of the flap's free end. As shown in this figure, the result with the number of iterations fixed at two is hardly distinguishable from that with the number of iterations fixed at three, while that with the number of iterations fixed at one diverged after it oscillated.

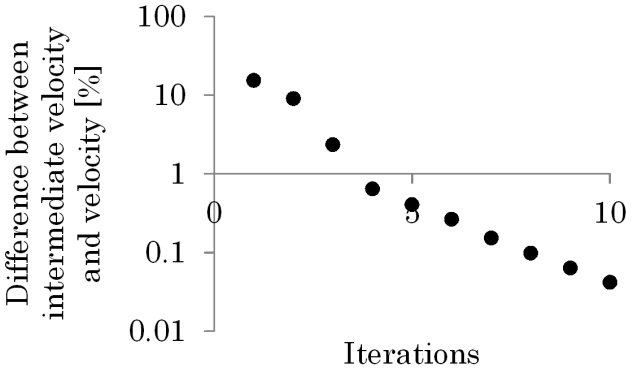

Figure 3: Transition of the difference between the intermediate velocity and the velocity during the iterative procedure at the first time step.

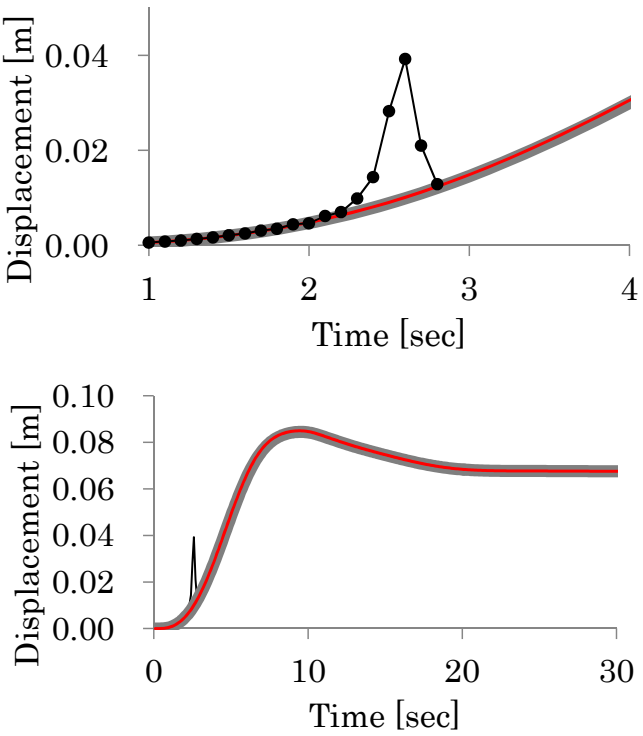

Figure 4: Time histories of the horizontal displacement of the flap's free end. The gray line indicates the result for three iterations, the red line indicates the result for two iterations, and the black line and circles indicate the result for no iteration.

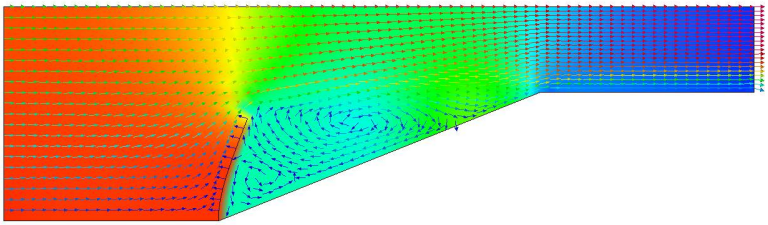

Figure 5: The fluid velocity and pressure fields in the channel, and the deformation of the flap at a time of 24 sec. The magnitude of the pressure is expressed as a color contour from blue (-0.5 Pa) to magenta (10 Pa), and the magnitude of the velocity is expressed as the color of the vector from blue (0 m/sec) to magenta (0.15 m/sec).

Therefore, two iterations are sufficient for the proposed method, which is less than the number of iterations required for some of sophisticated methods in the previous studies [Neumann et al. (2006); Idelsohn et al. (2009); Minami and Yoshimura (2010)]. It follows from this result that the proposed method is computationally efficient.

Fig. 5 shows the fluid velocity and pressure fields of the channel and the structural deformation of the flap. The results shown in Figs. 4 and 5 are in good agreement with those shown in the previous study [Neumann et al. (2006)].

5 Conclusions

We proposed a projection method for the monolithic interaction system of an incompressible fluid and a structure using a new algebraic splitting. The proposed method was based on the monolithic method in order to be strongly coupled, but split the monolithic equation system into the equilibrium equations and the PPE using the intermediate state variables algebraically in order to be computationally efficient. Different from the previous splitting using block-LU factorization or substructuring, the proposed splitting never produces any Schur complement.

The proposed method was applied for a channel with a flexible flap, which is one of typical test problems, in order to investigate its convergence properties, and the following results were obtained: Different from the monolithic method, the convergence property of the iterative solver for the proposed method was stable irrespective of the time increment of the analysis. The nonlinear iterations were linearly converged, and therefore, the PPE satisfied the incompressibility constraint asymp-

totically. Moreover, the number of nonlinear iterations for the convergence of the solution was far less than the number of coupled or nonlinear iterations required in some of sophisticated methods proposed in the previous studies. It follows from these results that the proposed method is computationally efficient.

Acknowledgement: This work was supported by JSPS KAKENHI Grant Number 23760078, JST A-STEP Grant Number AS251Z00433K and JSPS KAKENHI Grant Number 26390133.

References

Badia, S.; Nobile, F.; Vergara, C. (2008a): Fluid-structure partitioned procedures based on Robin transmission conditions. *Journal of Computational Physics*, vol. 227, pp. 7027-7051.

Badia, S.; Quaini, A.; Quarteroni, A. (2008b): Modular vs. non-modular preconditioners for fluid-structure systems with large added-mass effect. *Computer Methods in Applied Mechanics and Engineering*, vol. 197, pp. 4216-4232.

Badia, S.; Quaini, A.; Quarteroni, A. (2008c): Splitting methods based on algebraic factorization for fluid-structure interaction. *SIAM Journal on Scientific Computing*, vol. 30, pp. 1778-1805.

Bathe, K. J.; Dvorkin, E. N. (1985): A four-node plate bending element based on Mindlin/Reissner plate theory and a mixed interpolation. *International Journal for Numerical Methods in Engineering*, vol. 21, pp. 367-383.

Causin, P.; Gerbeau, J. F.; Nobile, F. (2005): Added-mass effect in the design of partitioned algorithms for fluid-structure problems. *Computer Methods in Applied Mechanics and Engineering*, vol. 194, pp. 4506-4527.

Chorin, A. J. (1968): Numerical solution of the Navier-Stokes equations. *Mathematics of Computation*, vol. 22, pp. 745-762.

Codina, R. (2001): Pressure stability in fractional step finite element methods for incompressible flows. *Journal of Computational Physics*, vol. 170, pp. 112-140.

Deparis, S.; Discacciati, M.; Fourestey, G.; Quarteroni, A. (2006): Fluid-structure algorithms based on Steklov-Poincare operators. *Computer Methods in Applied Mechanics and Engineering*, vol. 195, pp. 5797-5812.

Dettmer, W.; Peric, D. (2006): A computational framework for fluid-structure interaction: Finite element formulation and applications. *Computer Methods in Applied Mechanics and Engineering*, vol. 195, pp. 5754-5779.

Felippa, C. A.; Park, K. C.; Farhat, C. (2001): Partitioned analysis of coupled mechanical systems. *Computer Methods in Applied Mechanics and Engineering*,

vol. 190, pp. 3247-3270.

Fernandez, M. A. (2005): Moubachir, M. A Newton method using exact jacobians for solving fluid-structure coupling. *Computers and Structures*, vol. 83, pp. 127-142.

Fernandez, M. A.; Gerbeau, J-F.; Grandmont, C. (2007): A projection semi-implicit scheme for the coupling of an elastic structure with an incompressible fluid. *International Journal for Numerical Methods in Engineering*, vol. 69, pp. 794-821.

Forster, C.; Wall, W. A.; Ramm, E. (2007): Artificial added mass instabilities in sequential staggered coupling of nonlinear structures and incompressible viscous flows. *Computer Methods in Applied Mechanics and Engineering*, vol. 196, pp. 1278-1293.

Gerbeau, J. F.; Vidrascu, M. (2003): A quasi-Newton algorithm based on a reduced model for fluid-structure interaction problems in blood flows. *ESAIM: Mathematical Modelling and Numerical Analysis*, vol. 37, pp. 631-647.

Heil, M. (2004): An efficient solver for the fully coupled solution of large-displacement fluid-structure interaction problems. *Computer Methods in Applied Mechanics and Engineering*, vol. 193, pp. 1-23.

Hubner, B.; Walhorn, E.; Dinkler, D. (2004): A monolithic approach to fluid-structure interaction using space-time finite elements. *Computer Methods in Applied Mechanics and Engineering*, vol. 193, pp. 2087-2104.

Hughes, T. J. R.; Liu, W. K.; Zimmerman, T. K. (1981): Lagrangian-Eulerian finite element formulation for incompressible viscous flows. *Computer Methods in Applied Mechanics and Engineering*, vol. 29, pp. 329-349.

Idelsohn, S. R.; Del Pin, F.; Rossi, R.; Onate, E. (2009): Fluid-structure interaction problems with strong added-mass effect. *International Journal for Numerical Methods in Engineering*, vol. 80, pp. 1261-1294.

Ishihara, D.; Yoshimura, S. (2005): A monolithic approach for interaction of incompressible viscous fluid and an elastic body based on fluid pressure Poisson equation. *International Journal for Numerical Methods in Engineering*, vol. 64, pp. 167-203.

Ishihara, D.; Kanei, S.; Yoshimura, S.; Horie, T. (2008): Efficient parallel analysis of shell-fluid interaction problem by using monolithic method based on consistent pressure Poisson equation. *Journal of Computational Science and Technology*, vol. 2, pp. 185-196.

Ishihara, D.; Horie, T.; Denda, M. (2009a): A two-dimensional computational study on the fluid-structure interaction cause of wing pitch changes in dipteran

flapping flight. *The Journal of Experimental Biology*, vol. 212, pp. 1-10.

Ishihara, D.; Yamashita, Y.; Horie, T.; Yoshida. S.; Niho, T. (2009b): Passive maintenance of high angle of attack and its lift generation during flapping translation in crane fly wing. *The Journal of Experimental Biology*, vol. 212, pp. 3882-3891.

Knoll, D. A.; Keyes, D. E. (2004): Jacobian-free Newton-Lrylov methods: a survey of approaches and applications. *Journal of Computational Physics*, vol. 193, pp. 357-397.

Kuttler, U.; Wall, W. A. (2008): Fixed-point fluid-structure interaction solvers with dynamic relaxation. *Computational Mechanics*, vol. 43:61-72.

Le Tallec, P.; Mouro, J. (2001): Fluid structure interaction with large structural displacements. *Computer Methods in Applied Mechanics and Engineering*, vol. 190, pp. 3039-3067.

Matthies, H. G.; Steindorf, J. (2003): Partitioned strong coupling algorithms for fluid-structure interaction. *Computers and Structures*, 81:805-812.

Matthies, H. G.; Niekamp, R.; Steindorf, J. (2006): Algorithms for strong coupling procedures. *Computer Methods in Applied Mechanics and Engineering*, vol. 195, pp. 2028-2049.

Minami, S.; Yoshimura, S. (2010): Performance evaluation of nonlinear algorithms with line-search for partitioned coupling techniques for fluid–structure interactions. *International Journal for Numerical Methods in Fluids*, vol. 64, pp. 1129-1147.

Mok, D. P.; Wall, W. A. (2001): Partitioned analysis schemes for the transient interaction of incompressible flows and nonlinear flexible structures. *Trends in Computational Structural Mechanics. CIMNE: Barcelona*, pp. 689-698.

Nakata, T.; Liu, H. (2012): A fluid-structure interaction model of insect flight with flexible wings. *Journal of Computational Physics*, vol. 231, pp. 1822-1847.

Neumann, M.; Tiyyagura, S. R.; Wall, W. A. (2006): Robustness and efficiency aspects for computational fluid structure interaction. *Computational Science and High Performance Computing II*, vol. 91, pp. 99-114.

Noguchi, H.; Hisada, T. (1993): Sensitivity analysis in post-buckling problems of shell structures. *Computers and Structures*, vol. 47, pp. 699-710.

Perot, J. B. (1993): An analysis of the fractional step method. *Journal of Computational Physics*, vol. 10, pp. 51-58.

Rugonyi, S.; Bathe, K. J. (2001): On finite element analysis of fluid flows fully coupled with structural interactions. *Computer Modeling in Engineering and Sciences*, vol. 2, pp. 195-212.

Takizawa, K.; Tezduyar, T. E. (2012): Computational methods for parachute fluid-structure interactions. *Archives of Computational Methods in Engineering*, vol. 19, pp. 125-169.

Taylor, C. A.; Humphrey, J. D. (2009): Open problems in computational vascular biomechanics: hemodynamics and arterial wall mechanics. *Computer Methods in Applied Mechanics and Engineering*, vol. 198, pp. 3514-3523.

Tedzduyar, T. E.; Mittal, S.; Ray, S. E.; Shih, R. (1992): Incompressible flow computations with stabilized bilinear and linear equal-order-interpolation velocity-pressure elements. *Computer Methods in Applied Mechanics and Engineering*, vol. 95, pp. 221-242.

Washio, T.; Hisada, T.; Watanabe, W.; Tezduyar, T. E. (2005): A robust preconditioner for fluid-structure interaction problems. *Computer Methods in Applied Mechanics and Engineering*, vol. 194, pp. 4027-4047.

Yamada, T.; Yoshimura, S. (2008): Line search partitioned approach for fluid-structure interaction analysis of flapping wing. *Computer Modeling in Engineering and Sciences*, vol. 24, pp. 51-60.

Zhang, Q.; Hisada, T. (2001): Analysis of fluid-structure interaction problems with structural buckling and large domain changes by ALE finite element methods. *Computer Methods in Applied Mechanics and Engineering*, vol. 190, pp. 6341-6357.

Zhang, Q.; Hisada, T. (2004): Studies of the strong coupling and weak coupling methods in FSI analysis. *International Journal for Numerical Methods in Engineering*, vol. 60, pp. 2013-2029.